Inter-Decadal Modulations in the Dynamical State of the Kuroshio Extension System: 1905-2015

Bo Qiu, Shuiming Chen, and Niklas Schneider

Department of Oceanography, University of Hawaii at Manoa

Introduction

After separating from the Japanese coast at 36°N, 141°E, the Kuroshio enters the open basin of the North Pacific, where it is renamed the Kuroshio Extension (KE). Free from the constraint of coastal boundaries, the KE has been observed to be an eastward-flowing inertial jet accompanied by large-amplitude meanders and energetic pinched-off eddies (see, e.g., Qiu, 2002a for a comprehensive review). Compared to its upstream counterpart south of Japan, the KE is accompanied by a stronger southern recirculation gyre (RG) that increases the KE's eastward volume transport to more than twice the maximum Sverdrup transport (~60Sv) in the subtropical North Pacific Ocean, enhancing its nonlinear nature as a western boundary current extension. In addition to the high level of mesoscale eddy variability, an important feature emerging from recent satellite altimeter measurements and eddy-resolving ocean model simulations, is that the KE system exhibits clearly-defined decadal modulations between a stable and an unstable dynamic state (e.g., Qiu, 2003; Qiu & Chen, 2005, 2010; Taguchi et al., 2007, 2010; Cebollas et al. 2009; Sugimoto and Hanawa, 2009; Kelly et al. 2010; Sasaki et al., 2013). As shown on the cover page of this Exchanges issue, the KE paths were relatively stable in 1993–1995, 2002–2005 and 2010-2015. In contrast, spatially convoluted paths prevailed during 1996–2001 and 2006–2009. It is important to emphasize that these changes in path stability are merely one manifestation of the decadally-modulating KE system. When the KE jet is in a stable dynamic state, available satellite altimeter data further reveal that its eastward transport and latitudinal position tend to be greater and more northerly, its southern RG tends to strengthen, and the regional eddy kinetic energy level tends to decrease. The reverse is true when the KE jet switches to an unstable dynamic state.

KE index during the satellite era

To succinctly summarize the time-varying dynamical state of the KE system, Qiu et al. (2014) introduced the KE index defined as average of the variance-normalized time series of the southern RG intensity, the KE's intensity, its latitudinal position, and negative of its path length. A positive KE index, thus defined, indicates a stable dynamical state and a negative KE index, an unstable dynamical state. The red line in Figure 1c shows the KE index in the satellite altimetry period of 1993–2015. Dominance of the decadal modulation in the KE system is easily discernible in this time series. Transitions between the KE's two dynamical states are caused by the basin-scale wind stress curl forcing in the eastern North Pacific related to the Pacific decadal oscillations (PDOs). Specifically, when the central North Pacific wind stress curl anomalies are positive (i.e. positive PDO phase), enhanced Ekman flux divergence generates negative local sea surface height (SSH) anomalies in 170°–150°W along the southern RG latitude (see Figures 1a and 1b). As these wind-induced negative SSH anomalies propagate westward as baroclinic Rossby waves into the KE region after a delay of 3–4 years, they weaken the zonal KE jet, leading to an unstable (i.e., negative index) state, of the KE system with a reduced recirculation gyre and an active eddy kinetic energy field. The negative, anomalous wind stress curl forcing during the negative PDO phase, on the other hand, generates positive SSH anomalies through the Ekman flux convergence in the eastern North Pacific. After propagating into the KE region in the west, these anomalies stabilize the KE system by increasing the KE transport and by shifting its position northward, leading to a positive index state.

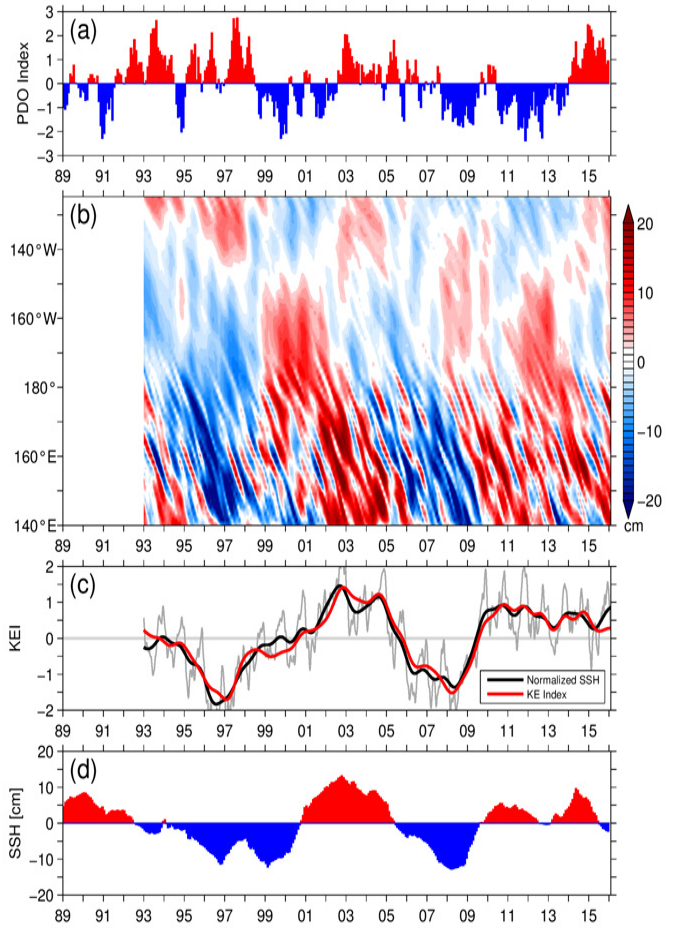

Figure 1: (a) Time series of Pacific decadal oscillation (PDO) from http://jisao.washington.edu/pdo/PDO.latest. (b) SSH anomalies along the zonal band of 32°-34°N from the AVISO satellite altimeter data. (c) Time series of the KE index synthesized from four dynamical properties (red line) versus the normalized SSH anomalies averaged in 31°-36°N and 140°-165°E (black lines); here, the thin black line denotes the weekly time series and the thick black line the low-pass filtered time series. (d) SSH anomalies in the 31°-36°N and 140°-165°E box predicted by the 1.5-layer reduced-gravity model forced by the ECMWF Interim wind stress data.

A regression analysis in Qiu et al. (2014) reveals that the KE index defined by the 4 dynamical properties can be favourably represented by the sea surface height (SSH) signals inside the KE's southern RG region of 31°–36°N and 140°–165°E (black lines in Figure 1c). The linear correlation coefficient between the two red and thick (thin) black lines in Figure 1c is as high as 0.97 (0.84). Physically, this high correlation is of little surprise because the large-scale KE variability is closely entwined to the dynamical state of its southern RG and the RG's variability is well represented by its regional SSH signals. On a practical level, this makes exploration of the KE dynamical state be equivalent to examination of the SSH signals in the key region of the KE's southern RG.

As evidenced in Figure 1b, changes in the mid-latitude wind-forced SSH field is governed by westward-propagating Rossby wave adjustment processes (see Qiu, 2002b, and references therein, for theoretical justification). Figure 1d shows the SSH time series averaged in the 31°–36°N and 140°–165°E box based on the 1.5-layer reduced-gravity model forced by the monthly ECMWF ERA-Interim wind stress data (Dee et al., 2014). The correlation between this modelled SSH time series and that shown in Figure 1c (thick black line) reaches 0.85, demonstrating the usefulness of the wind-forced 1.5-layer reduced-gravity model in capturing the decadal modulations of the KE dynamical state during the past quarter of a century.

KE index over the past century

Use of the SSH signals in the southern RG box as a proxy for the KE dynamical state allows us to explore the KE index variations beyond the satellite altimetry era. To achieve this, we merge the ECMWF reanalysis wind stress product ERA-20C (available from 1900 to 2010; Stickler et al., 2014) and ERA-Interim (available from 1979 to 2015) and force the 1.5-layer reduced-gravity model (over the overlapping period of 1979-2010, the merge is done bi-linearly). Figure 2a shows the model-derived SSH changes in the KE's southern RG box of 31°–36°N and 140°–165°E. Notice that to focus on the decadal variability, we have removed the long-term increasing linear trend of 1.5 cm/decade from Figure 2a; also, no SSH signals are evaluated in the first 5 years due to the model spin-up. For comparison and serving as an independent check, we plot in Figure 2b the time series of surface dynamic height calculated from the historical, objectively-analyzed, T/S data compiled by Ishii et al. (2006) in the same southern RG box from 1945 to 2012. Because the available T/S data is confined to the upper ocean of 1,500m, the amplitude of the T/S-based KE index is, on average, about half that derived from the wind-forced 1.5-layer reduced-gravity model. However, the observed phase changes of the KE index agree well with those predicted by the wind-forced model hindcast. Note that the agreement between Figures 2a and 2b improves after 1960s when the in-situ T/S measurements became more abundant: the linear correlation coefficient between the two time series in 1960–2012 is 0.82, as compared to 0.74 during the overlapping period of 1945–2012.

Both Figures 2a and 2b reveal that the low-frequency modulation of the KE dynamical state is not confined to the last two decades during which we had satellite-based SSH information to capture the detailed evolution of the KE system. To examine how the dominant period of the century-long KE index has modulated over the past century, we plot in Figure 2c the wavelet power spectrum for the KE index time series shown in Figure 2a. Large-amplitude decadal changes can be seen to persist after the mid-1970s. From mid-1940s to mid-1970s, the KE index appears to have two dominant periods: one in the 15~20-year band and the other in the 4~6-year band. Note that the short 4~6-year variability in the KE index was also detected in the eddy-resolving OFES model output of 1955–1975 that was forced by the NCEP-NCAR reanalysis wind stress data (Qiu et al., 2014; their Figure 5a). In between the mid-1920s and mid-1940s, the KE index appears to be dominated by the 10~15-year fluctuations and prior to the mid-1920s, Figure 2c indicates that the predominant period of the time-varying KE index falls in between 6 and 10 years.

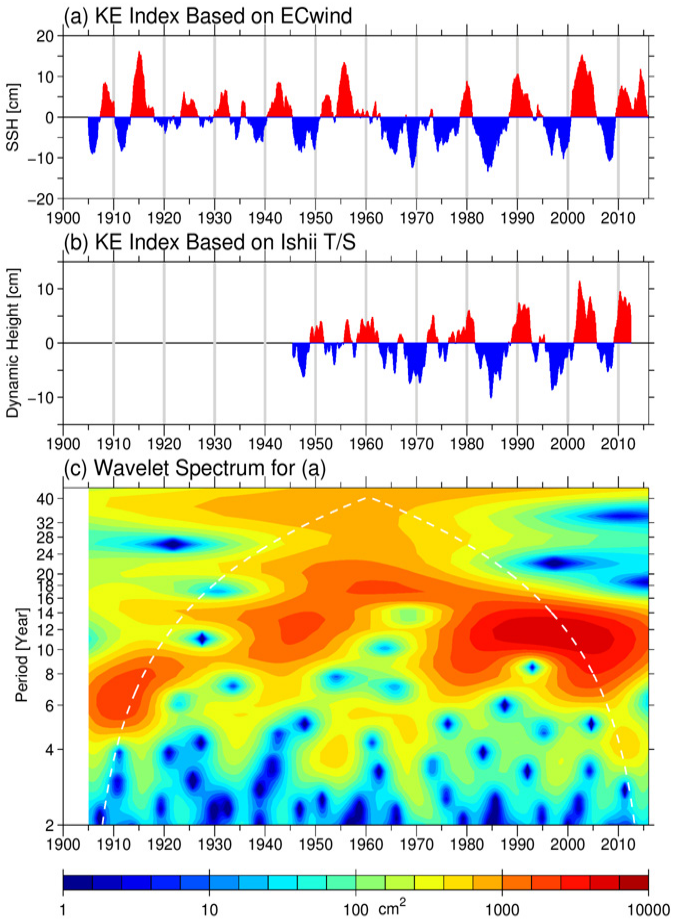

Figure 2: (a) KE index time series based on the SSH anomalies in the 31°-36°N and 140°-165°E box predicted by the 1.5-layer reduced-gravity model forced by the merged ERA-20C and Interim wind stress data. (b) KE index time series based on the SSH anomalies in the 31°-36°N and 140°-165°E box calculated from the historical T/S data of Ishii et al. (2006). Notice the difference from (a) in y-axis scale. (c) Wavelet power spectrum for the time series of (a).

It is worth emphasizing that the mid-1920s, mid-1940s, and mid-1970s marked the three 20th-century climatic regime shifts in the Aleutian Low pressure system over the North Pacific Ocean (e.g., Minobe, 1997; Zhang et al., 1997). The results in Figure 2 clearly indicate that these regime shifts in the atmospheric forcing field exert a significant impact upon the frequency content of the time-varying KE system. What is yet to be explored and quantified is the degree to which the variability in the KE dynamical state may feedback to the low-frequency changes in the overlying atmospheric circulation. By transporting warmer tropical water to the mid-latitude ocean, the expansive KE provides a significant source of heat and moisture for the North Pacific mid-latitude atmospheric storm tracks (e.g., Nakamura et al., 2004). By modifying the path and intensity of the wintertime overlying storm tracks, changes in the KE dynamic state can alter not only the stability and pressure gradient within the local atmospheric boundary layer, but also the basin-scale wind stress pattern (Taguchi et al., 2009; Kwon et al., 2010; Frankignoul et al., 2011; Kwon and Joyce, 2013). After the latest regime shift of the mid-1970s, Qiu et al. (2007; 2014) show that a positive (negative) index KE state tends to generate a positive (negative) wind stress curl in the eastern North Pacific basin, resulting in negative

(positive) local SSH anomalies through Ekman divergence (convergence). This impact on wind stress induces a delayed negative feedback with a preferred period of ~10 years and is likely the cause for the enhanced decadal variance demonstrated in Figure 2. It will be important for future studies to clarify if similar feedback mechanisms are at work within the epochs of other climatic regime shifts in the 20th century.

Acknowledgments

The ERA-Interim and ERA-20C surface wind stress data are provided by ECMWF and the merged satellite altimeter data by the Copernicus Marine and Environment Monitoring Service (CMEMS). Support from NASA NNX13AE51G and NSF OCE-0926594 is acknowledged.

References

Ceballos, L., E. Di Lorenzo, C. D. Hoyos, N. Schneider, and B. Taguchi, 2009: North Pacific Gyre oscillation synchronizes climate variability in the eastern and western boundary current systems. J. Climate, 22, 5163-5174.

Dee, D. P., M. Balmaseda, G. Balsamo, R. Engelen, A. J. Simmons, and J.-N. Thépaut, 2014: Toward a Consistent Reanalysis of the Climate System. Bull. Amer. Meteor. Soc., 95, 1235-1248.

Frankignoul, C., and N. Sennéchael, Y.-O. Kwon, and M.A. Alexander, 2011: Influence of the meridional shifts of the Kuroshio and the Oyashio Extensions on the atmospheric circulation. J. Climate, 24, 762-777.

Kelly, K.A., R.J. Small, R.M. Samelson, B. Qiu, T.M. Joyce, Y.-O. Kwon and M.F. Cronin, 2010: Western boundary currents and frontal air-sea interaction: Gulf Stream and Kuroshio Extension. J. Climate, 23, 5644-5667.

Kwon, Y.-O., and T.M. Joyce, 2013: Northern hemisphere winter atmospheric transient eddy heat fluxes and the Gulf Stream and Kuroshio-Oyashio Extension variability. J. Climate, 26, 9839-9859.

Kwon, Y.-O., M. A. Alenxader, N. A. Bond, C. Frankignoul, H. Nakamura, B. Qiu, and L. Thompson, 2010: Role of the Gulf Stream and Kuroshio-Oyashio Systems in large-scale atmosphere-ocean interaction: A review. J. Climate, 23, 3249-3281.

Ishii, M., M. Kimoto, K. Sakamoto, and S.-I. Iwasaki, 2006: Steric sea level changes estimated from historical ocean subsurface temperature and salinity analyses. J. Oceanogr., 62, 155-170.

Minobe, S., 1997: A 50–70 year climatic oscillation over the North Pacific and North America. Geophys. Res. Lett., 24, 683-686.

Nakamura, H., T. Sampe, Y. Tanimoto, and A. Shimpo, 2004: Observed associations among storm tracks, jet streams and midlatitude oceanic fronts. Earth's Climate: The Ocean-Atmosphere Interaction, Geophys. Monogr., 147, Amer. Geophys. Union, 329-346.

Qiu, B., 2002a: The Kuroshio Extension system: Its large-scale variability and role in the midlatitude ocean-atmosphere interaction. J. Oceanogr., 58, 57-75.

Qiu, B., 2002b: Large-scale variability in the midlatitude subtropical and subpolar North Pacific Ocean: Observations and causes. J. Phys. Oceanogr., 32, 353-375.

Qiu, B., 2003: Kuroshio Extension variability and forcing of the Pacific decadal oscillations: Responses and potential feedback. J. Phys. Oceanogr., 33, 2465-2482.

Qiu, B., and S. Chen, 2005: Variability of the Kuroshio Extension jet, recirculation gyre and mesoscale eddies on decadal timescales. J. Phys. Oceanogr., 35, 2090-2103.

Qiu, B., and S. Chen, 2010: Eddy-mean flow interaction in the decadally modulating Kuroshio Extension system. Deep-Sea Res. II, 57, 1098-1110.

Qiu, B., N. Schneider, and S. Chen, 2007: Coupled decadal variability in the North Pacific: An observationally-constrained idealized model. J. Climate, 20, 3602-3620.

Qiu, B., S. Chen, N. Schneider, and B. Taguchi, 2014: A coupled decadal prediction of the dynamic state of the Kuroshio Extension system. J. Climate, 27, 1751-1764.

Sasaki, Y. N, S. Minobe and N. Schneider, 2013: Decadal response of the Kuroshio Extension jet to Rossby waves: Observation and thin-jet theory. J. Phys. Oceanogr., 43, 442-456.

Stickler, A., S. Brönnimann, M. A. Valente, J. Bethke, A. Sterin, S. Jourdain, E. Roucaute, M. V. Vasquez, D. A. Reyes, R. Allan, and D. Dee, 2014: ERA-CLIM: Historical Surface and Upper-Air Data for Future Reanalyses. Bull. Amer. Meteor. Soc., 95, 1419-1430.

Sugimoto, S., and K. Hanawa, 2009: Decadal and interdecadal variations of the Aleutian Low activity and their relation to upper oceanic variations over the North Pacific. J. Meteor. Soc. Japan, 87, 601-614.

Taguchi, B., H. Nakamura, M. Nonaka, and S.P. Xie, 2009: Influences of the Kuroshio/Oyashio Extensions on air-sea heat exchanges and storm-track activity as revealed in regional atmospheric model simulations for the 2003/04 cold season. J. Climate, 22, 6536-6560.

Taguchi, B., S.-P. Xie, N. Schneider, M. Nonaka, H. Sasaki, and Y. Sasai, 2007: Decadal variability of the Kuroshio Extension. Observations and an eddy-resolving model hindcast. J. Climate, 20, 2357-2377.

Taguchi, B., B. Qiu, M. Nonaka, H. Sasaki, S.-P. Xie, and N. Schneider, 2010: Decadal variability of the Kuroshio Extension: mesoscale eddies and recirculations. Ocean Dyn., 60, 673-691.

Zhang, Y., J. M. Wallace, and D. S. Battisti, 1997: ENSO-like Interdecadal Variability: 1900–93. J. Climate, 10, 1004-1020.